

## Supplementary Information

### Supplementary Figure Legend

Supplementary Figure 1.

*Experimental set up and confirmation of Rab1 conformation of yeast nucleus arrested in G1 and M.*

**a)** At collection for Hi-C analysis an aliquot of cells was fixed and DNA stained with DAPI. Only experiments that had >94% large budded cells were taken for further processing. Budding index demonstrates CDK activation in yeast cells. Mitotic cells were then assessed as to whether they had maintained the pre-anaphase arrest – as indicated by a single nucleus. Or had proceeded into anaphase – as indicated by 2 split nuclei. Abbreviations for states are as used in text specifically **M** - *cdc20* arrested, **MH** – cohesin depleted (*scc1-73*) *cdc20* arrested, **MD** – condensin depleted (*smc2td GAL1-smc2K38I*) *cdc20* arrested. R1 and R2 refer to replicate 1 and replicate 2, respectively. Therefore two independent experiments were conducted for each state.

**b)** Telomeres (40kb) of all chromosome arms have been grouped according to arm length. The interaction frequency between the 8 shortest and 8 longest arms relative to each other has been analyzed.

**c)** Zoom into contact heatmaps from G1 and M datasets for selected regions on (top) ChrXV (0-330kb (CENXV is at 330kb)) and (bottom) the post-rDNA region of ChrXII (660 kb to 940 kb). Each block represents 10kb bin.

**d)** Zoom into log<sub>2</sub> ratio of M over G1 contact maps for selected regions on (top) ChrXV (0-330kb (CENXV is at 330kb)) and (bottom) the post-rDNA region of ChrXII (660 kb to 940 kb).

**e)** Overlaid P(s) curves for each individual chromosome arm taken from G1 (green) or M (blue) cells. All contact maps shown were assembled from two independent experiments.

Supplementary Figure 2.

*Mitotic chromosome conformation can be accounted for by addition of intra-chromosomal loops, but not by sister-crosslinks.*

- a)** The family of P(s) curves for 150 loops, and a range of different coverage levels (left). And the family of P(s) curves for coverage=0.4, and a range of number of loops (right).
- b)** Simulations with sister-crosslinks imposed with the indicated frequency (12kb, 192kb, none) at random positions along chromosome arms in different simulations. Importantly, sister-crosslink simulations do not display two phases in their P(s), unlike experimental M-phase P(s) curves (grey, two replicas).

Supplementary Figure 3.

*Mitotic chromosome compaction requires cohesin function.*

- a)** (Top) Zoom into contact heatmaps from MH data for selected regions on (left) ChrXV (0-330kb (CENXV is at 330kb)) and (right) the post-rDNA region of ChrXII (660 kb to 940 kb).  
(Bottom) Zoom into log<sub>2</sub> ratio of MH over M contact maps for selected regions on (left) ChrXV (0-330kb (CENXV is at 330kb)) and (right) the post-rDNA region of ChrXII (660 kb to 940 kb).
- b)** (Left) Log<sub>2</sub> (MH/M) ratio of contacts for ChrXII. Regions where contact frequency was higher in MH (-cohesin) than M (wt cohesin) are shown in red, regions where contact frequency was lower in MH than M in blue. The post-rDNA region is highlighted by the orange bar.  
(Right) Contact probability, P(s), as a function of genomic separation, s, specifically for the post-rDNA region of ChrXII for the replicate experiments of MH and M.
- All contact maps shown were assembled from two independent experiments.

Supplementary Figure 4.

*Cohesin-dependent compaction is independent of sister chromatid cohesion.*

- a)** FACS for DNA content (left) and Western blotting (right) showing that *cdc45* and *cd45 scc1-73* cells enter mitosis without DNA replication, with CDK phosphorylating condensin on Smc4 Serine 4 (Smc4 S4P) with the same kinetics as wildtype cells (\*unspecific band). Picture of Ponceau stained blot confirms equal loading of Western (right, bottom). Western blotting for to confirm CDK activation in cells was from one experiment.

**b)** Plot of nuclear morphology examining number of DAPI stained cells from the indicated timepoints that have undergone nuclear division. % of single nucleus (rectangles), double nuclei (checked line with squares) and cells with an anaphase nucleus are shown (grey line).

**c)** (Top) Zoom into contact heatmaps from *cdc45* mitotically arrested cells, C, (top) and cohesin depleted mitotically arrested cells, CH, (bottom), for selected regions on (left) ChrXV (0-330kb (CENXV is at 330kb)) and (right) the post-rDNA region of ChrXII (660 kb to 940 kb).

**d)** Zoom into log<sub>2</sub> ratio of CH over C contact maps for selected regions on (left) ChrXV (0-330kb (CENXV is at 330kb)) and (right) the post-rDNA region of ChrXII (660 kb to 940 kb). Arrows indicate a prominent track of cohesin-dependent contacts seen also in supplementary Fig. 3a).

All contact maps shown were assembled from two independent experiments.

Supplementary Figure 5.

*Mitotic conformation following depletion of Smc2 and characterization of smc2K38I allele.*

**a)** (Left) Hi-C data collected from M phase cells following disruption of conDensin with *smc2td* allele to deplete Smc2 (MD*smc2*). Chromosomes XIII to XVI are shown as representative of the whole genome. (Middle) Log<sub>2</sub> ratio of *smc2* depleted M dataset over *wt* M dataset (MD*smc2*/M), respectively. (Right) P(s) of M versus MD*smc2*. Data set assembled from one Hi-C data set.

**b)** Description and characterization of the *smc2td GAL1smc2K38I* allele used in Figures 5 and 6. **i)**

Western blot showing degradation of the degron tagged Smc2 protein and the concurrent GAL1 induced expression of Smc2K38I mutant in both nocodazole and *cdc20* arrested metaphase state.

Expression examined by Western blot in one experiment **ii)** FACS analysis of DNA content following degradation of *smc2td* with/without expression of Smc2K38I. Representative profiles shown from one of two independent experiments. Expression of Smc2K38I increases the aneuploidy of cells generated following one cell division (right) as shown by increased number of cells with more than 2C and less than 1C DNA content. Profiled cells also contain V5-tagged Brn1 (as in (iii)). **iii)** ChIP analysis of condensin complex enrichment as assayed by ChIP with Brn1-V5 at *CEN4*, in wildtype cells (*wt*) (average of n=11), *smc2* degron cells (*smc2-td*) (average of n=5), or *smc2-td* combined with expression of *smc2K38I* (average of n=3) shown in a boxplot format with all data points shown. The

mean of each boxplot indicated by horizontal bar. The increased penetrance of the *smc2K38I* phenotype with regard to aneuploidy and chromatin binding suggests that this allele approximates the null state. CHIP reactions were performed in one set of experiments.

**c)** (Left) Zoom into contact heatmaps from condensin depleted mitotically arrested cells, MD, for ChrXV (0-330kb (CENXV is at 330kb)). (Right) Zoom into log<sub>2</sub> ratio of MD over M contact maps for ChrXV (0-330kb (CENXV is at 330kb))

Supplementary Figure 6.

*Changes between in cis and in trans tRNA-tRNA loci contacts in the different datasets.*

**a)** The map of average contact probability between tRNA pairs located on the same chromosomal arm and separated by 80kb-120kb. To avoid indirect clustering effects, we selected tRNA-tRNA pairs located more than 100kb away from a centromere or a telomere (90 pairs in total).

**b)** Same as in **(a)**, but for tRNA pairs located on the same chromosomal arm, but separated by 180kb-220kb (50 pairs in total).

**c)** Same as in **(a)** and **(b)**, but for tRNA pairs located on different chromosomes (8290 pairs in total).

**d)** Speculative models of how cohesin complexes have a dual role in both generating chromatin loops *in cis* and sister chromatid cohesion *in trans*.

Cohesin complexes act in chromatin loop formation and sister chromatid cohesion independently. In this model distinct populations of cohesin complexes are engaged in chromatin loop formation and sister chromatid cohesion. We speculate that loop forming complexes will exhibit dynamic binding of chromatin whereas cohesive cohesin complexes will be stably bound to chromatin.

**e)** Cohesin complexes could simultaneously act in sister chromatid cohesion and in loop formation. This model would require that both cohesive and non-cohesive complexes could promote chromatin loops. In the “handcuff” model of cohesive cohesin this would require two loop-promoting cohesin complexes being brought together.

## Supplementary Table legends

*Supplemental Table 1. Summary of Hi-C libraries constructed during this study.*

R1 and R2 refer to Replicate 1 and Replicate 2 respectively

*Supplemental Table 2. Yeast strains and genotypes used during this study*

Full genome wide shotgun sequencing of strains used available on request

### **Supplementary Table 1– Summary of Hi-C libraries generated in this study**

Full details of libraries and raw sequencing available at GEO number: GSE87311

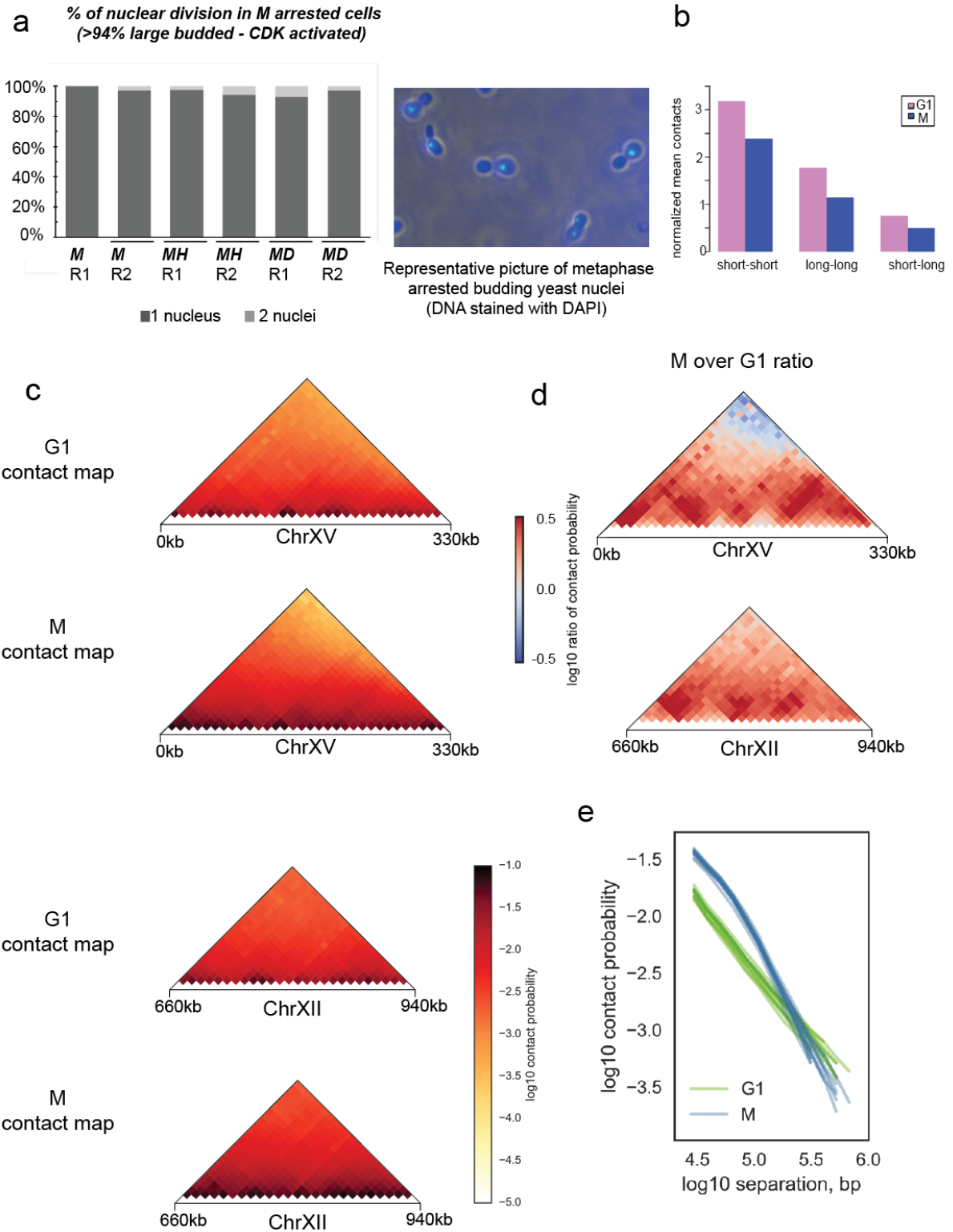
Sample	Total reads from each side	unique valid pairs
wt G1 R1	241,459,680	52,249,342
wt G1 R2	245,245,920	75,685,505
wt M R1	192,027,518	64,944,673
wt M R2	427,487,395	85,672,725
MH R1	56,917,488	23,371,565
MH R2	166,890,033	57,512,008
MDsmc2 R1	111,130,137	44,619,350
MD R1	232,928,309	88,073,200
MD R2	196,668,125	74,468,608
C R1	71,309,748	20,264,415
C R2	246,282,342	95,845,558
CH R1	64,251,477	15,532,255
CH R2	245,646,429	95,363,974

Abbreviations for libraries (also used in main text): **M** - *cdc20* arrested, **MH** – cohesin depleted (*scc1-73*) *cdc20* arrested, **MDsmc2** condensin depleted *cdc20* arrested, (*smc2td*) **MD** – condensin depleted and *smc2k38I* expressed (*smc2td GAL1-smc2k38I*) *cdc20* arrested, **C** – *cdc45-td* mitotic arrest (nocodazole) and **CH** *cdc45-td* and *scc1-73* mitotic arrest (nocodazole). R1 and R2 refer to replicate 1 and replicate 2 respectively.

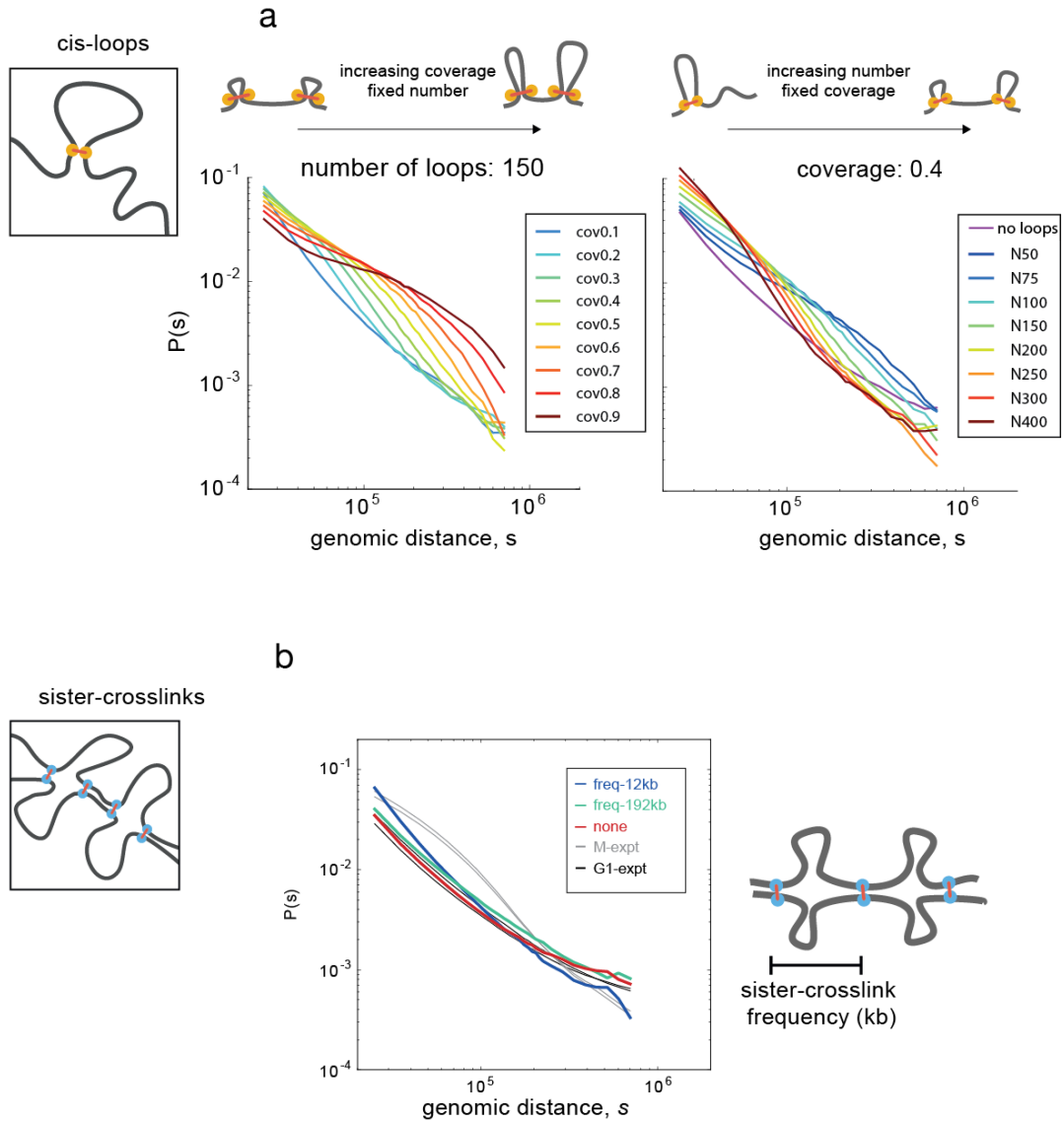
**Supplementary Table 2– Yeast strains and genotypes**

<i>cdc20-td</i> (wt)	MATa <i>ade2-1 ura3-1 his3-11, trp1-1, can1-100</i> UBR1::pGAL-myc-UBR1 (HIS3), <i>leu2-3 LEU2::pCM244 x3</i> <i>cdc20-td</i> CDC205' upstream -100 to -1 replaced with kanMX-tTA (tetR-VP16)-tetO2 - Ub -DHFRts - Myc -linker)
<i>scc1-73 cdc20-td</i>	<i>cdc20-td</i> + <i>scc1-73 TRP1</i>
<i>smc2td GAL1-SMC2K38I cdc20-td</i>	<i>cdc20-td</i> + SMC2 5' upstream -100 to -1 replaced with kanMX-tTA (tetR-VP16)-tetO2 - Ub -DHFRts - 3xHA extended linker), <i>trp1-1::pFA6 TRP1- GAL1-SMC2-K38I-HA-TRP1</i>
<i>smc2td</i>	<i>cdc20-td</i> + SMC2 5' upstream -100 to -1 replaced with kanMX-tTA (tetR-VP16)-tetO2 - Ub -DHFRts - 3xHA extended linker)
<i>cdc45-td</i> <sup>A0</sup>	UBR1::pGAL-myc-UBR1 (HIS3), CDC45::cdc45-td (CUP1p-Ub-DHFRts-HA-CDC45)(TRP1)
<i>cdc45-td scc1-73</i>	UBR1::pGAL-myc-UBR1 (HIS3), CDC45::cdc45-td (CUP1p-Ub-DHFRts-HA-CDC45)(TRP1), <i>scc1-73, trp1::hphNT1</i>

Supplementary Figure 1. Related to Figure 1  
 Experimental set up and Hi-C conformation  
 in budding yeast cells arrested in G1 and M



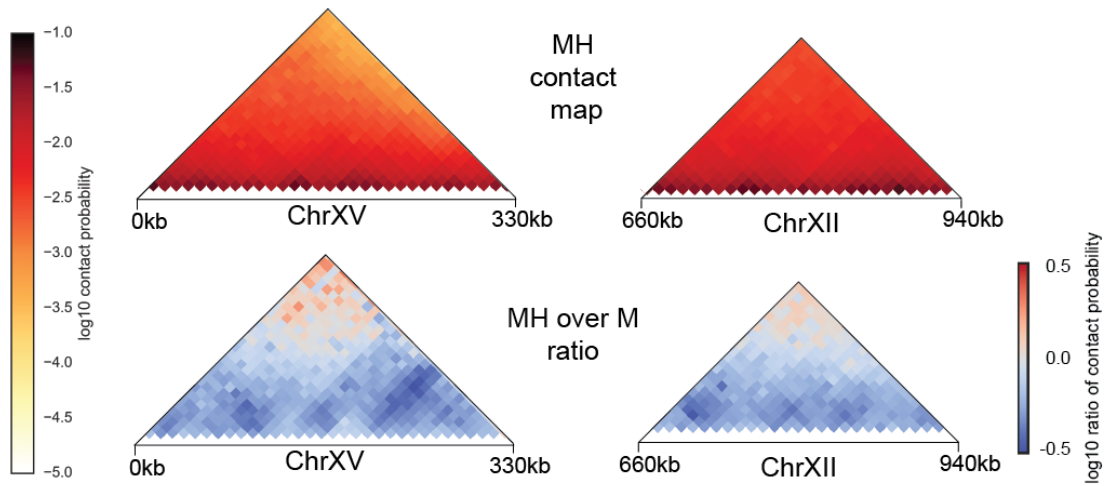
Supplementary Figure 2. Related to Figure 2;  
 Mitotic chromosome conformation can be accounted for by addition  
 of intra-chromosomal loops, but not by sister-crosslinks.



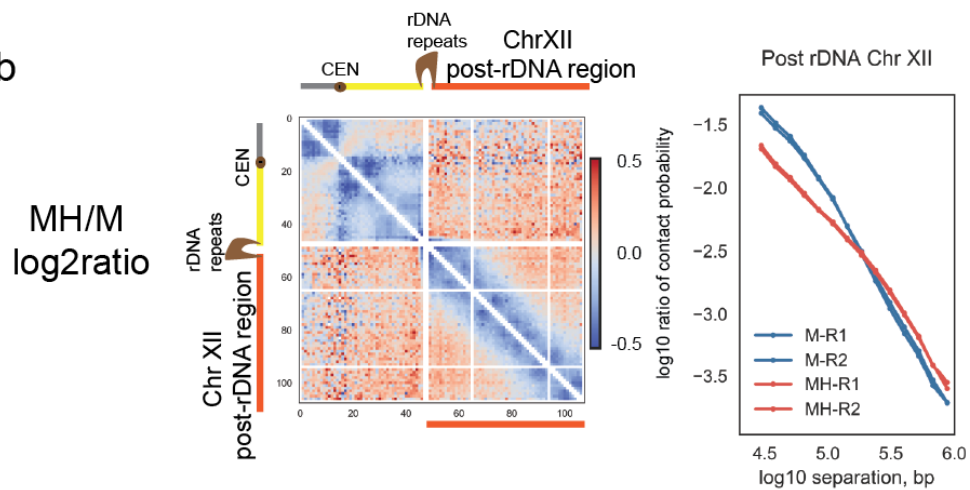


Supplementary Figure. 3 related to Figure 3.  
 Mitotic chromosome compaction requires cohesin function

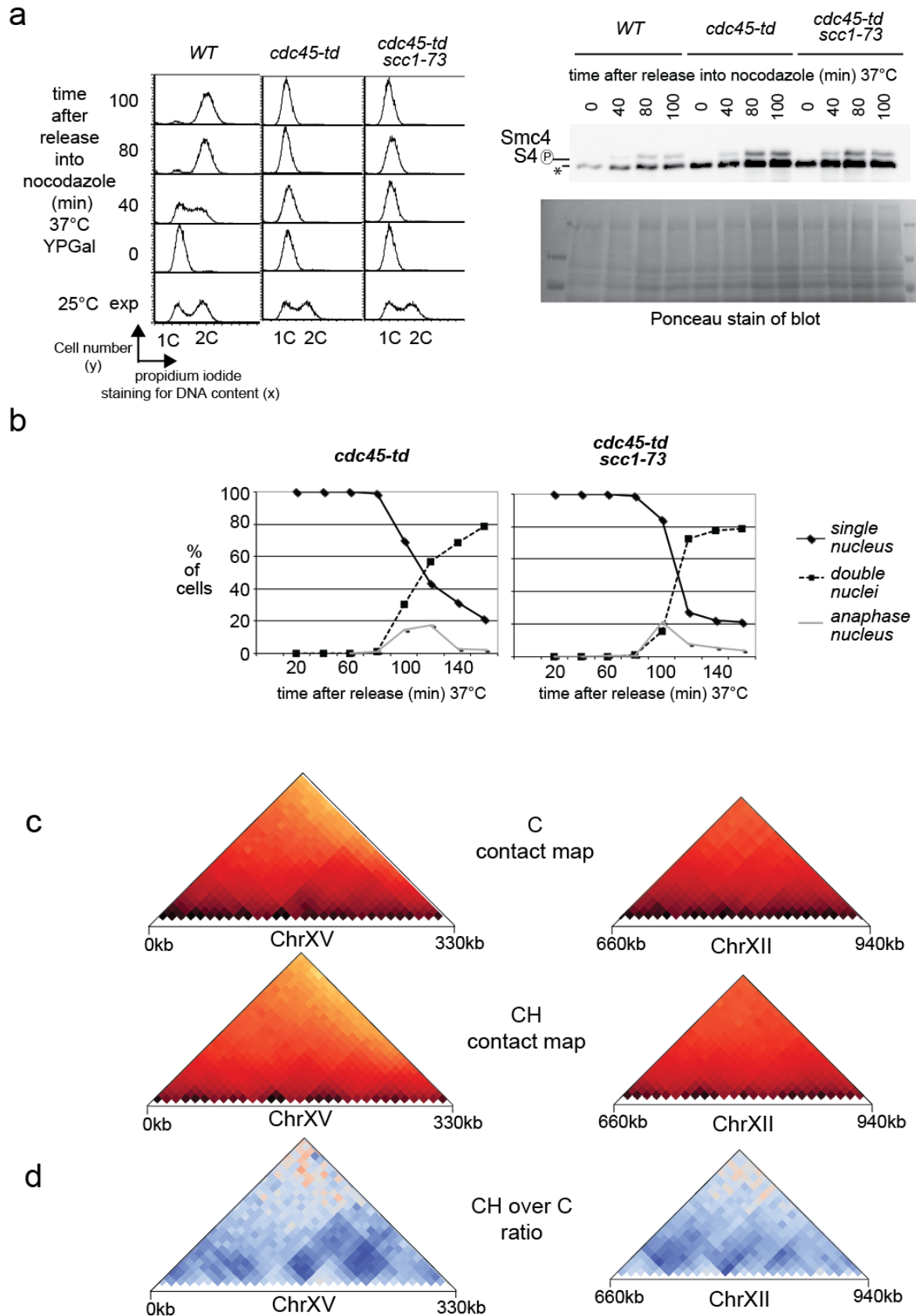
a



b

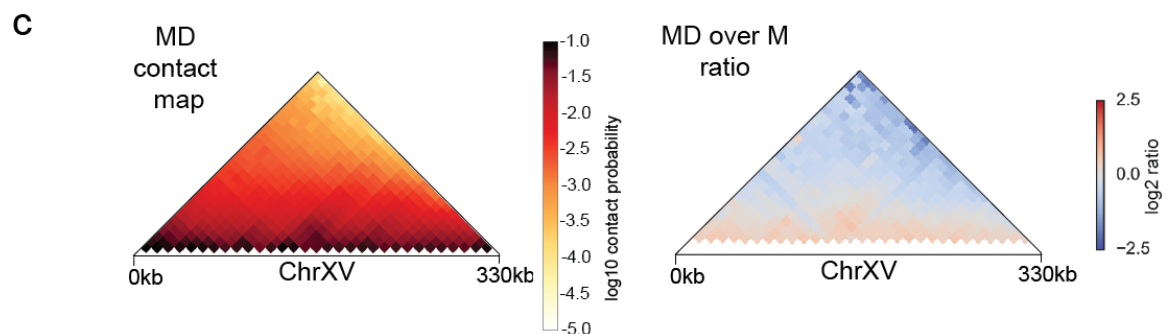
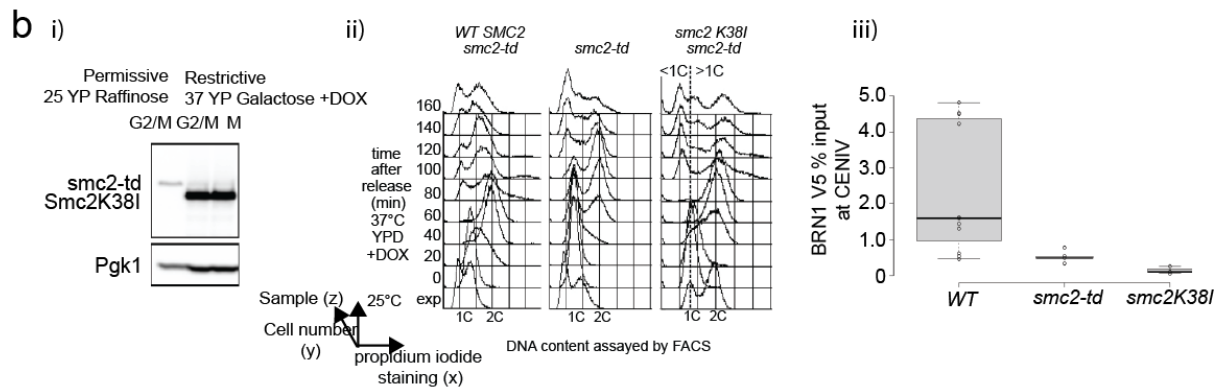
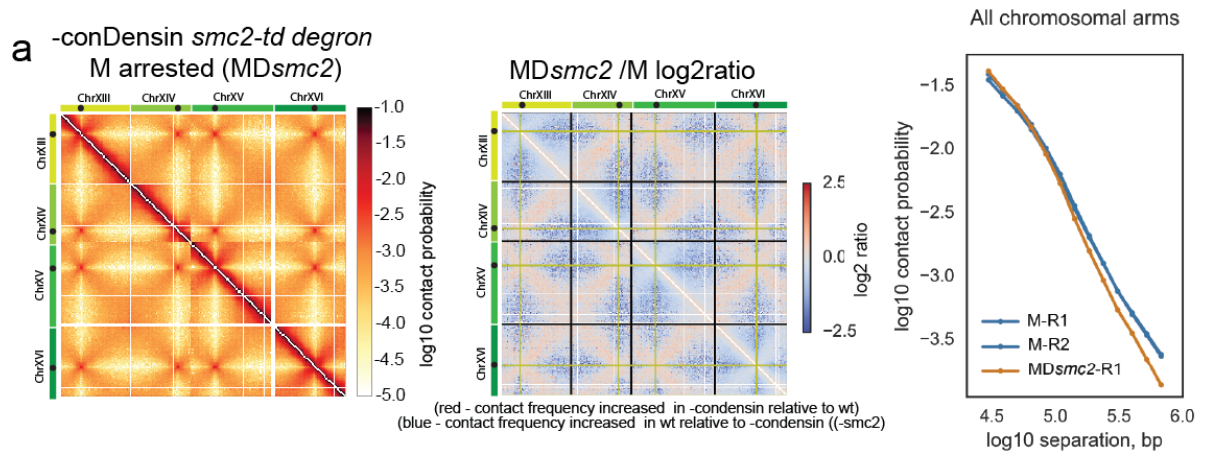


Supplementary Figure. 4 related to Figure 4.  
 Cohesin dependent compaction is independent of sister chromatid cohesion



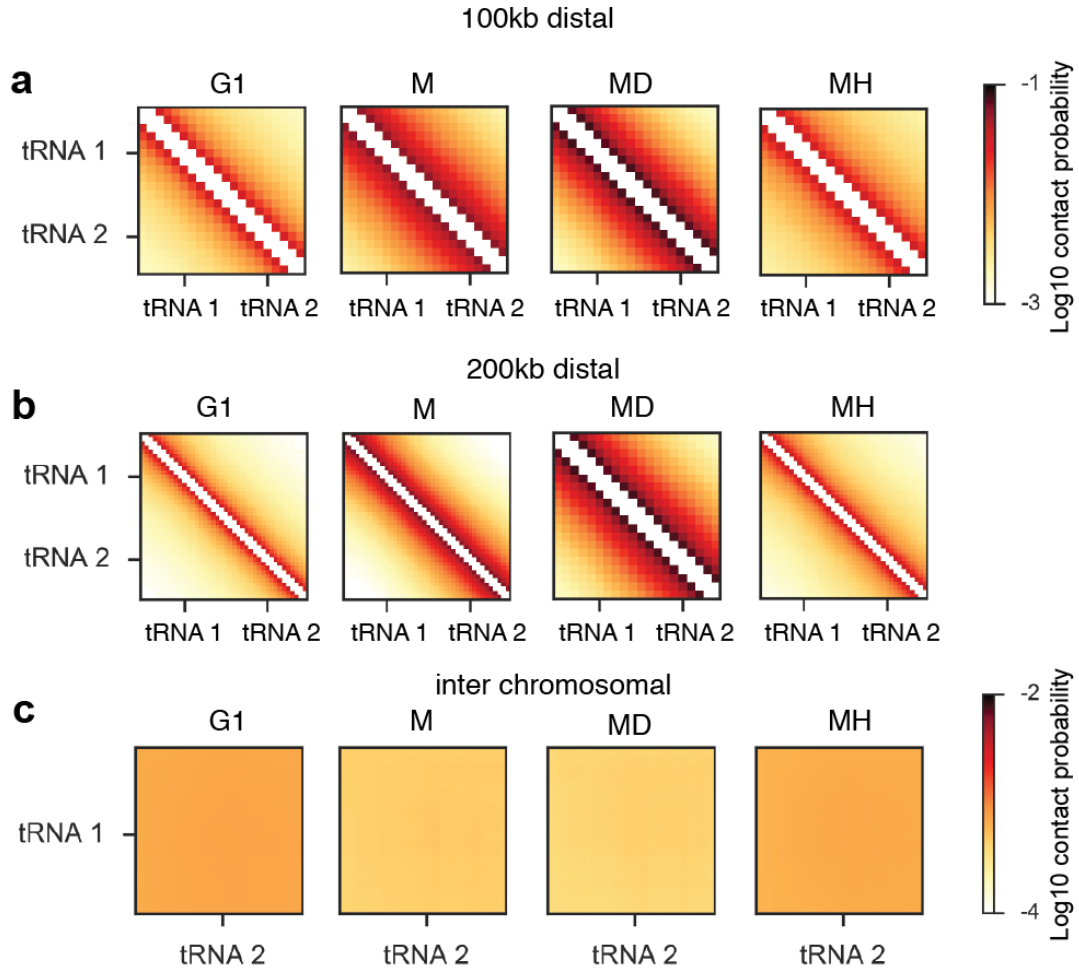
## Supplementary Figure 5

### Mitotic conformation following depletion of Smc2 and characterization of *SMC2K38I* allele



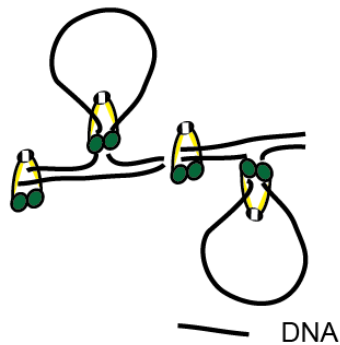
## Supplementary Figure 6

### Changes between *in cis in trans* tRNA - tRNA loci contacts in the different datasets

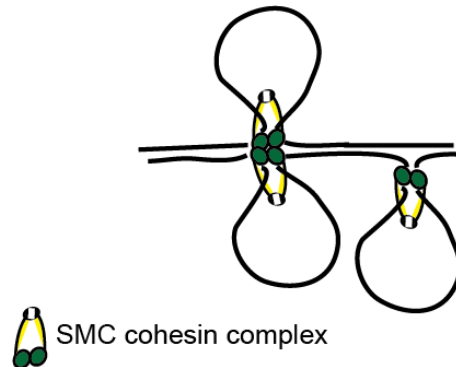


Hypothetical models of cohesin activity in chromatin looping and sister chromatid cohesion

**d** Chromatin loop formation independent of sister chromatid cohesion



**e** Chromatin loop formation occurs alongside sister chromatid cohesion



## **Methods**

### ***Statistics and reproducibility***

No statistical methods were used to predetermine sample size. The replicates of the conditions are shown individually for all P(s) histograms. For contact heatmaps data from replicates was pooled. Details of individual libraries available in Supplementary Table 1. Number of times each condition tested is indicated in each figure legend.

### ***Yeast Strains***

Yeast strains were derived from W303-1a (*MATa ade2-1 ura3-1 his3-11, trp1-1 leu2-3, can1-100*) adapted for use with the degron system. Full details in Supplemental Table 2.

### ***Media and cell cycle synchronization for Hi-C experiments***

Yeast cells were grown in YP + 2% Glucose at 25 °C, transferred to YP + 2% Raffinose (YPR) and grown over night to log phase. Cells were then arrested in G1 with 10 µg/ml alpha factor until 90% of cells were unbudded (120 min). The cells were washed three times with YPR and released in YPR. After 30 min 10 µg/ml of nocodazole was added and budding was checked after 1h. After cells entered G2 (60-70 min after release), Galactose at 2% final concentration and 15 min later Doxycycline at 50µg/ml final concentration were added. 30 min after addition of Galactose, the temperature was shifted to 37 °C. Cells were grown at 37 °C for 1h and then washed three times in YPR + Galactose + Doxycycline and released in the same media to allow spindles to reform in cells depleted of Cdc20. Cells were then collected after 30 min for *cdc20* metaphase arrest.

### ***Cell fixation and Hi-C library preparation***

Carried out as described<sup>63</sup> with the variation that cells were fixed at 37 °C. Conditions and number of replicates used for each state shown in Table S1.

### ***FACS, Nuclear morphology, Western blotting and Antibodies used***

Carried out as described<sup>64</sup>. Smc4 phosphoS4 antibody was a kind gift from Damien D'Amours<sup>35</sup>. Anti-HA antibody (12Ca5 mouse monoclonal IgG<sub>2β</sub>K. Roche, Fisher scientific 10026563). Anti-V5 antibody (MCA1360, abD Serotec) used for ChIP.

### ***Chromatin Immunoprecipitation (ChIP)***

Fixed cells were defrosted and re-suspended in 100 µl ChIP buffer (150 mM NaCl, 50 mM Tris HCl, 5mM EDTA, 0.5 % NP-40 (IGEPAL), 7 % Triton X-100, cOmplete Tablets, Mini EDTA-free EASYpack (Roche). Cells were lysed in a FASTPREP machine, 6 rounds of 30 seconds at 6.5 power, with 1 ml of 0.5 mm silica beads. The bottom lysate spun out and resuspended in 1ml ChIP buffer. Sonicated for 15x 30 seconds (Biorupter Pico, Diagenode). 100 µl of sonicate was processed as an input control, 200 µl was incubated with 12.5µg/ml anti-V5 antibody (MCA1360, abD Serotec). For immuno-precipitation (IP) tubes were agitated for an hour and a half at 4°C. 45µl magnetic beads, (Dynabeads protein G – Life Technologies), washed 3 times in 1ml ChIP buffer were added and tubes incubated at 4°C for 2 hours.

Magnetic beads were isolated and washed four times in ChIP buffer, and a fifth time in ChIP buffer minus protease-inhibiting supplement. To reverse cross-linking, magnetic beads were incubated with 10% Chelex100 resin beads (BioRad 142-1253), in purified water at 95°C for 30 min. Samples were spun down and the supernatant kept at -20°C prior to analysis by qPCR. Input controls were precipitated using 0.1x vol 3M NaAC pH5.2 and 2.5 x vol 100% EtOH and then cross-linking reversed as above, before purification with Nucleospin PCR clean up kit and eluted in nuclease-free purified water.

The immune-precipitated DNA was analysed using 2X AB-1323/B ABsolute™

QPCR SYBR. Green Low ROX Mix and processed in an MX3005p qPCR machine. Primers used for RT-PCR of DNA at CENIV are (forward) TGCTTGCAAAGGTCACATGCTTAT and (reverse) CATTTTGGCCGCTCCTAGGTAGTG.

. Data was analysed using the ‘Percentage Input Method’ where the CT values obtained from the ChIP are divided by the CT values obtained from the Input control samples. Since 1% of starting chromatin was used for each input sample, in order to adjust the CT value of input samples to 100% 6.644 (log<sub>2</sub> of 100) was subtracted from it. Then the following formula was used to calculate the percentage input for each IP sample:

$2^{(\text{adjusted ChIP input CT value} - \text{IP CT value})} \times 100.$

### ***Computational Analysis of Hi-C maps***

#### ***Mapping and filtering contacts***

We mapped sequenced read pairs to W303 yeast genome using Bowtie 2.1.0 and the previously described method of iterative mapping<sup>27</sup>. To generate contact lists, we assigned each mapped side to a *HindIII* fragment and removed the contacts with both sides assigned to the same *HindIII* fragment, reads with one unmapped side as well as PCR duplicates, i.e. identical contact pairs.

### ***Aggregating contact maps***

To generate Hi-C contact maps, we aggregated the filtered contact lists into 10kb genomic bins using the *cooler* Python package for Hi-C data analysis, publicly available at <https://github.com/mirnylab/cooler/>. We filtered out low coverage genomic bins using the MAD-max (maximum allowed median absolute deviation from the median coverage) filter on the total number of interactions per bin, set to 7.4 median absolute deviations (corresponding to 5 standard deviations in the case of a normal distribution). We also removed the contacts within the first two diagonals of the contact maps as they are contaminated by uninformative Hi-C artifacts, unligated and self-ligated DNA fragments. Finally, we iteratively corrected the resulting maps to equalize genomic coverage.

### ***Contact map analyses***

We calculated the curves of intra-arm contact probability  $P(s)$  vs genomic separation,  $s$ , from the 10kb contact maps using 15 logarithmically spaced bins<sup>27</sup> spanning distances between 20kb to 1Mb. We excluded Chromosomes IV and XII from these analyses as well as the bins within 40kb distance from the nearest centromere and telomere. The post-rDNA scalings were generated using the same approach on the region between the rDNA locus on chromosome XII and the telomere of the corresponding arm. We generated the centromere and tRNA pile-ups by averaging the contact maps of regions surrounding the respective genomic features. To exclude a possible contribution of telomeric conformations, we only used genomic features that were separated from the telomeres by more than 200kb.

### ***Polymer models***

We modeled the yeast genome as 16 polymers, subject to additional constraints imposed by yeast chromosome organization, and intra-chromosomal loops generated specified number and coverage (Fig. 2 a-e). We then obtained conformations from simulations and calculated simulated contact maps. For a range of looping parameters, intra-arm  $P(s)$  was calculated from these contact maps and

compared with experimental  $P(s)$  to determine the best-fitting parameter sets for each experimental condition.

### ***Polymer Fiber***

Following<sup>31</sup> we simulate the yeast genome as 16 chromatin fibers of 20nm monomers, each monomer representing 640bp (~4 nucleosomes). Polymer connectivity was implemented by connecting adjacent monomers with harmonic bonds using a potential  $U = 100*(r - 1)^2$  (energy in units of kT, distances in monomers). The stiffness of the fiber was implemented using a three point interaction term, with the potential  $U = 2.5*(1-\cos(\alpha))$ . Excluded volume interactions between monomers were implemented using a soft-core repulsive potential with a maximum repulsion  $U(0)=1.5$  that goes to zero at a distance of 1.05 (i.e.  $U(1.05) = 0$ ), as in<sup>4</sup>.

### ***Geometric constraints***

Geometric constraints were implemented as in<sup>30</sup> with slight modifications:

- i.* Confinement to the nucleus: harmonically increasing potential (1kT /monomer) when monomer radial position exceeds the confinement radius (1000nm).
- ii.* Centromere tethering to the SPB: centromeres were confined to a spherical volume (radius of 250nm) with a harmonically increasing potential (1kT /monomer) when monomer radial position exceeds the confinement radius.
- iii.* Tethering of telomeres to the nuclear periphery: telomeres were subject to a harmonic potential pushing them to the periphery (1kT/monomer distance) when their radial position was less than .95 of the nucleus radius.
- iv.* Repulsion from the nucleolus: monomers entering the nucleolus were subject to a harmonically increasing potential (1kT/monomer distance). Both sides of the rDNA locus on chromosome XII were attracted to the periphery of the nucleolus, imposed with harmonic potentials (1kT/monomer distance).

### ***Intra-chromosomal loops***

To generate sets of intra-chromosomal (*cis*-) loops with a desired coverage and number, we used 1D loop extrusion simulations (see<sup>4,34</sup>) using a genome-wide lattice at monomer resolution with boundaries at chromosome telomeres, centromeres, and the rDNA locus on chrXII. This ensures that



loops are generated within chromosomes, are non-overlapping, do not cross centromeres, or link two regions together on opposite sides of the rDNA locus. Note that other than these requirements, we allow positions of loops to be variable along the chromosome arm. In polymer simulations, intra-chromosomal loops are then imposed with harmonic bonds (as in <sup>4,65</sup>).

### ***Code Availability***

All libraries used for analysis and simulations are publically available at

<https://bitbucket.org/mirnylab/hiclib> and <https://bitbucket.org/mirnylab/openmm-polymer>

### ***Data availability statement***

Full details of libraries and raw sequencing available at GEO number: GSE87311. Genomic sequencing of each test strain available from the authors on request. All data that support the conclusions are available from the corresponding author on reasonable request.

### **References for methods**

63. Belton, J.-M. & Dekker, J. Hi-C in Budding Yeast. *Cold Spring Harb Protoc* **2015**, 649–661 (2015).
64. Baxter, J. & Diffley, J. F. Topoisomerase II inactivation prevents the completion of DNA replication in budding yeast. *Molecular Cell* **30**, 790–802 (2008).
65. Goloborodko, A., Imakaev, M. V., Marko, J. F. & Mirny, L. Compaction and segregation of sister chromatids via active loop extrusion. *Elife* **5**, e14864 (2016).